ACS OMEGA

Open Access

http://pubs.acs.org/journal/acsodf

Article

Antimicrobial and Superhydrophobic CuONPs/TiO_2 Hybrid Coating on Polypropylene Substrates against Biofilm Formation

Sudipto Pal,* Stefania Villani, Antonella Mansi, Anna Maria Marcelloni, Alessandra Chiominto, Ilaria Amori, Anna Rita Proietto, Matteo Calcagnile, Pietro Alifano, Sonia Bagheri, Claudio Mele, Antonio Licciulli, Alessandro Sannino, and Christian Demitri*

Cite This: *ACS Omega* 2024, 9, 45376−45385

Read Online

ACCESS | Metrics & More | Article Recommendations | Supporting Information

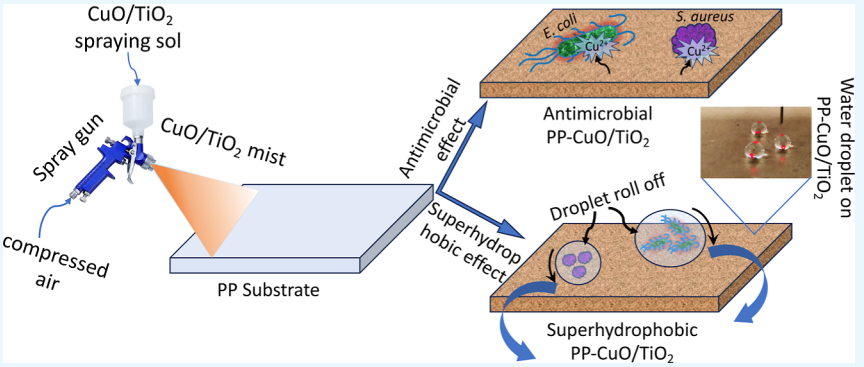

ABSTRACT: Biofilm formation in common public places and hospitals is of great concern. Active antimicrobial coatings can prevent the formation of bacterial biofilms and the spreading of primary and secondary infections caused by contagious bacteria and viruses. In the present work, we report a simple spray coating process using copper oxide (CuO) nanoparticles (NPs) dispersed in a titanium dioxide (TiO_2) sol, where CuONPs act as the active antimicrobial agent and TiO_2 as the inorganic binder. Homogeneous CuONPs/TiO_2 coating was obtained on polypropylene substrates by spraying the CuO/TiO_2 sol using a commercial air gun, followed by drying at 80 °C. The amount of CuONPs loading in the coating was adjusted by controlling the number of coated layers. CuONPs and CuONPs/TiO_2 coatings were characterized by XRD, BET, X-ray fluorescence spectroscopy, AFM, and field emission scanning electron microscopy techniques. All of the coated films showed dual activity, i.e., antimicrobial and superhydrophobicity. A high bactericidal effect against both *Escherichia coli* and *Staphylococcus aureus* was observed for the coated substrates. Coatings with higher CuONPs showed greater antibacterial activity, reaching *R* value >6, and no bacterial colonies were detected after 24 h of incubation. An increasing trend of water contact angle was observed with the increasing amount of CuONP loading.

1. INTRODUCTION

The great incidence of microbial infections, together with the risky exposure of patients and healthcare workers to frequently touched surfaces in hospitals and public places, raises the need to develop efficient and cost-effective biocidal coatings.[1−5] The formation of biofilms, a common strategy adopted by the microorganisms to increase the bacterial resistance to environmental stress and antibacterial treatments, is of great concern.[1,6,7] Additionally, due to the emergence of the COVID-19 pandemic, there was an upsurge in the production of antimicrobial and antiviral agents, such as floor/hand sanitizers, wet wipes, sprays, and personal care and cleaning products that are not only costly but also create adverse health issues, including acute respiratory diseases, due to the incorporation of several hazardous chemical compounds (alcohol ∼70%, sodium hypochlorite, hydrogen peroxide, quaternary ammonium compounds, etc.).[2−4] Therefore, it is of high importance to develop effective coating strategies that could prevent the formation of bacterial biofilms thanks to their higher biocidal activity and, at the same time, would be favorable to the environment. Nanomaterials, such as copper (Cu), silver (Ag), gold (Au), zinc (Zn), and magnesium (Mg), and metal oxides, like titanium dioxide (TiO_2), zinc oxide (ZnO), and cerium oxide (CeO_2) are widely used as antimicrobial agents because of their well-known antibacterial

Received: August 9, 2024
Revised: August 27, 2024
Accepted: September 2, 2024
Published: October 29, 2024

properties.[8−14] Among them, Cu and Ag, either in metallic or oxide form, are well-known biocidal compounds due to their superior broad-spectrum antimicrobial activity for decades.[13,15−17] Although there are ongoing debates on their biocidal actions due to the complex mechanism of the antibacterial/antiviral pathways, Cu-based nanomaterials possess a higher biocidal action over Ag-based ones, and this aspect has been demonstrated against a wide range of pathogenic microorganisms.[18−22]

Cu nanoclusters and their oxide counterparts, cuprous oxide (Cu_2O) and cupric oxide (CuO), have shown superior antimicrobial activities against a wide range of pathogens like *Escherichia coli*, *Staphylococcus aureus*, *Bacillus subtilis*, *Legionella pneumophila*, and some fungi and viruses, including SARS-CoV-2, thanks to the contact-killing mechanism.[2,15,17,19,20,23−27] Although it is reported that Cu_2O nanomaterials show stronger antimicrobial activity compared to CuO due to the higher oxidation state, CuO is thermodynamically more stable and less reactive than Cu_2O when mixed with other materials favoring the coating formulation.[23,28] On the other hand, bacterial adhesion and biofilm formation on various surfaces could be minimized by applying a superhydrophobic coating having a higher water contact angle (WCA) with lower rolling angle values, and the same might be achieved by applying colloidal silica-based superhydrophobic coatings.[29,30] However, a superhydrophobic coating itself cannot prevent the transmission of microbial agents unless the bacteria are killed within a specific time frame before they are transmitted. Therefore, the addition of an antibacterial agent to the coating matrix is strongly recommended. There are several strategies to prepare antimicrobial Cu-based coatings, such as chemical vapor deposition, physical vapor deposition, electrophoretic deposition, electron beam evaporation, electroless plating, sputtering, plasma-spraying, thermal spray coating, sol−gel coating method, etc.[8,31−33] Among the strategies reported above, the sol−gel method is considered one of the most promising and inexpensive coating techniques that can be applied over a wide variety of substrates, especially when a large area has to be covered.[16,34] Some recent studies demonstrate the antibacterial activity of $Cu/CuO_x/TiO_2$ against several pathogens, but there are some drawbacks in these works, either complexity in coating formulation or moderate antibacterial efficiency that limits their practical applications, especially where large areas need to be protected.[35−39] Herein, we report an easy and upscalable spray coating strategy based on the commercially available CuONPs in powder form dispersed in a sol−gel-derived TiO_2 sol. Smooth polypropylene (PP) sheets were coated with CuONPs/TiO_2 sol using a commercial spray gun. CuONPs and CuO-based coatings were characterized by scanning electron microscopy (SEM), XRD, atomic force microscopy (AFM), and water contact angle (WCA) measurements. The antibacterial efficacy of the coated specimens was tested against reference bacterial strains according to the ISO 22196:2011 standards.

2. MATERIALS AND METHODS

2.1. Reagents. All of the reagents were used as received without any modifications. Copper(II) oxide, nanopowder (CuO, 30−50 nm APS Powder, denoted as CuONPs), and hydrochloric acid (HCl, 37%) were purchased from Alfa-Aesar, whereas titanium tetra-isopropoxide (TTIP, 97%) and ethanol (ACS reagent grade, 99.9%) were purchased from Sigma-Aldrich.

2.2. Coating Preparation. CuONPs/TiO_2 coating was deposited on PP substrates by a two-step coating process. At first, the TiO_2 coating was deposited by the spray coating method. The TiO_2 sol (containing 5% of TiO_2 by weight in ethanol) was prepared by hydrolysis−condensation of TTIP in the presence of HCl and deionized water (Millipore Milli Q). The molar ratios of the reagents were TTIP/HCl/H_2O = 1:0.5:4. At first, TTIP was added dropwise to ethanol and stirred for 10 min. After homogeneous mixing of the solution, the required amount of HCl previously diluted with water was added to the above solution. The sol was stirred for several hours to complete the hydrolysis−condensation reaction. The as-prepared sol was aged for 1 day before the coating application. The cleaned PP substrates (50 × 50 × 2 mm dimension) were coated with the TiO_2 sol by spraying method using a commercially available manual stainless-steel spray gun (nozzle size 1.5 mm, fitted with a 600 mL PP feed cup). The spray gun was connected to a compressed air pump to maintain an air pressure of 2 bar in order to achieve a uniform coating. After coating deposition, the PP substrates were kept in an oven at 80 °C for one night to gently dry the coated film and avoid any unwanted cracks. To prepare the CuONPs/TiO_2 coating, at first, CuO/TiO_2 sol was prepared. CuO nanopowder (0.5 wt %) was dispersed in 1 wt % TiO_2 sol (diluted from the 5 wt % mother sol using ethanol as the solvent) under ultrasonication and stirred overnight to prepare a well-dispersed sol. This sol was then applied to the TiO_2-coated PP substrates by a spray coating method. CuONPs/TiO_2-coated PP substrates were kept in an oven at 80 °C to promote the adherence of CuONPs to the substrates. The amount of CuONPs loading on the TiO_2-coated PP substrates was controlled by choosing the number of spray coating layers applied with the CuONPs/TiO_2 sol. According to the elemental quantification estimated from the X-ray fluorescence spectroscopy (XRF) measurements (discussed later), the coated samples are assigned as TCuO-1 (∼1 wt % CuO), TCuO-2 (∼2 wt % CuO), and TCuO-5 (∼5 wt % CuO), whereas TiO_2 indicates coating with the base layer with TiO_2 and PP as the PP sheets.

2.3. Characterization of CuO-Based Coatings. X-ray diffraction analysis was performed with a Rigaku Ultima X-ray diffractometer using Cu Kα radiation (λ = 1.5406 Å) operating at 40 kV/20 mA with a step size of 0.02°. Morphological characterization of the coating was carried out on a Zeiss Sigma VP field emission scanning electron microscope. Specific surface area and pore size distribution of CuONPs were measured by the Brunauer−Emmett−Teller (BET) method from the N_2 adsorption−desorption curve using an Anton Parr NOVA 2200e surface area analyzer. The concentration of CuONPs deposited with respect to TiO_2 was estimated from quantitative elemental analysis using the XRF technique performed with an M4 TORNADO Micro-XRF spectrometer (Bruker Nano, Berlin, Germany) operating at 50 kV/600 μA (30 W) equipped with an X-Flash solid-state silicon drift detector. Advanced polycapillary X-ray optics were used, which reduces the X-ray spot size to 25 μm, ensuring very high excitation intensity. Data acquisition was performed on different positions of the coated film in the area mode to cover a maximum possible area under scanning. The WCA on the coated and bare PP substrates was measured with an FTA 1000 series Goniometer (First Ten Angstroms, USA) using the

https://doi.org/10.1021/acsomega.4c07345
ACS Omega 2024, 9, 45376−45385

drop shape analysis technique. The surface topography and roughness of the coatings were analyzed using a Bruker Multimode 8 AFM in a quantitative nanomechanical mode under ambient conditions. Images were captured with scan sizes of 10 × 10 μm^2 with a scan rate of 0.6−0.7 Hz and an image resolution of 512 samples per line. A ScanAsyst-air cantilever (Bruker) with a resonance frequency of 70 kHz and a spring constant of 0.4 N/m was employed. Data processing was performed using Nanoscope Analysis software (version 1.5).

2.4. Antibacterial Activity Evaluation. The antibacterial efficacy of CuONPs coatings was assessed against *E. coli* (ATCC 8739) and *S. aureus* (ATCC 6538P). Bacteria were grown in nutrient broth (NB) at 37 °C. The composition of the NB medium was as follows: 3 g of meat extract, 10 g of peptone, and 5 g of sodium chloride in 1 L of bidistilled water. Nutrient agar (NA) plates were prepared by adding 15 g of agar per liter of NB. Laboratory tests to evaluate the antibacterial activity of the CuO-based coatings were performed according to the ISO 22196:2011 standard[40] with some adjustments.[41] For both tested bacterial strains, the preinoculum was prepared by making a suspension in 1/500 NB medium of an isolated colony grown on a NA plate incubated for 18−24 h at 35 ± 1 °C. The day after, the bacterial suspension was adjusted to reach a concentration between 2.5 × 10^5 and 1.0 × 10^6 Colony Forming Units per milliliter (CFUs/mL). Then, 0.4 mL of the bacterial suspension was deposited on untreated (PP) and treated (PP/TCuO-1; PP/TCuO-2; PP/TCuO-5) PP substrates. The antibacterial activity of all the specimens was evaluated immediately after the bacterial inoculum (T_0) and after 24 h (T_{24}) of incubation at 35 ± 1 °C. After being washed with 10 mL of D/E neutralizing broth (BD Difco), each specimen was subjected to bacterial cell recovery. Serial dilutions of the extraction solution were sown for inclusion on plates of Plate Count Agar (PCA, Oxoid Ltd.) in triplicate and then incubated at 35 ± 1 °C for 24−48 h.

According to ISO 22196:2011, the antibacterial activity is attributable to coatings capable of determining a reduction (R) in the number of bacterial colonies ≥2 logarithmic units per unit of surface (Log_{10} CFU/cm^2) within a contact time of 24 h. In our case, the R value was determined by calculating the average reduction value of the number of bacterial cells on the CuONPs-based coatings compared to those untreated following eq 1

$$R = (U_t - U_0) - (A_t - U_0) = U_t - A_t \quad (1)$$

where U_0 is the average of the common logarithm of the number of viable bacteria in CFUs/cm^2, recovered from the PP specimens immediately after inoculation (T_0); U_t is the average of the common logarithm of the number of viable bacteria in CFU/cm^2, recovered from the PP specimens after 24 h (T_{24}) of inoculation; A_t is the average of the common logarithm of the number of viable bacteria in CFU/cm^2, recovered from the PP/TCuO specimens after 24 h (T_{24}) of inoculation. For each condition, the experiments were performed in triplicate.

2.5. Statistical Analysis. The data are presented as the mean ± standard deviation for the indicated number of experiments. The statistical analysis was conducted by using a two-way ANOVA. In all comparisons, $p < 0.05$ was considered statistically significant, and the significance level was reported when present.

3. RESULTS AND DISCUSSION

The recent spread of antibiotic-resistant pathogens has accelerated the need to find new antimicrobial strategies that are not only bactericidal but also help reduce the spread of infections. In this context, hospital facilities play a fundamental role in the spread of antibiotic-resistant pathogens due to the intense use of broad-spectrum antibiotics. The objective of this research is therefore to develop a simple, economical, but effective coating strategy with antibiotic and antibiofilm activity, designed for the coating of plastic surfaces in daily use, which negatively affect the risk of contracting infections by operators and patients, such as light switches, handles, furniture, and commonly used accessories.

Prior to the coating formulation, the physicochemical properties of the CuONPs were screened by XRD, BET, and SEM measurements. Figure 1a shows the BET adsorption−desorption isotherm, which resulted in a type IV isotherm typical of mesoporous materials. From the BET equation, a surface area of 17.2 m^2/g was estimated, and an average pore diameter of 3.38 nm was obtained that remains within the mesoporous range. The SEM micrograph of the CuONPs is shown in Figure 1b, where the average size of the particles could be estimated to about 40 nm, which is very close to the

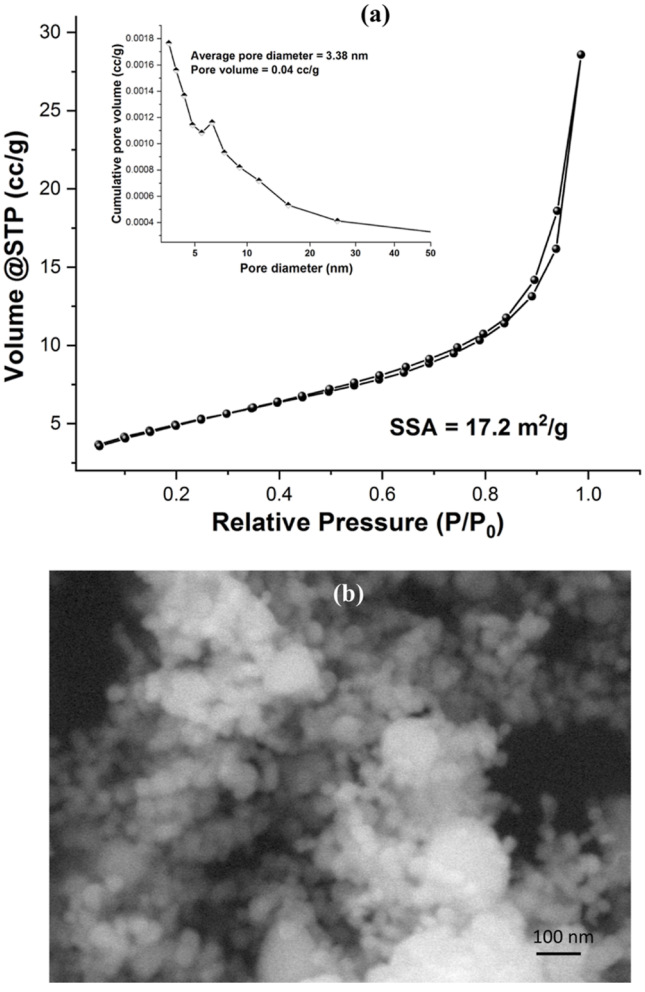

Figure 1. (a) N_2 adsorption−desorption isotherm and pore size distribution (inset of a) of the CuONPs and (b) FESEM micrograph of bare CuONPs.

https://doi.org/10.1021/acsomega.4c07345
ACS Omega 2024, 9, 45376−45385

reported one according to the technical data sheet from the supplier. It is also observed that the particles are uniformly dispersed without any significant agglomeration, favoring preparing a homogeneous suspension.

The crystalline phase of the CuONPs was investigated by recording the XRD pattern and is shown in Figure 2, where *hkl*

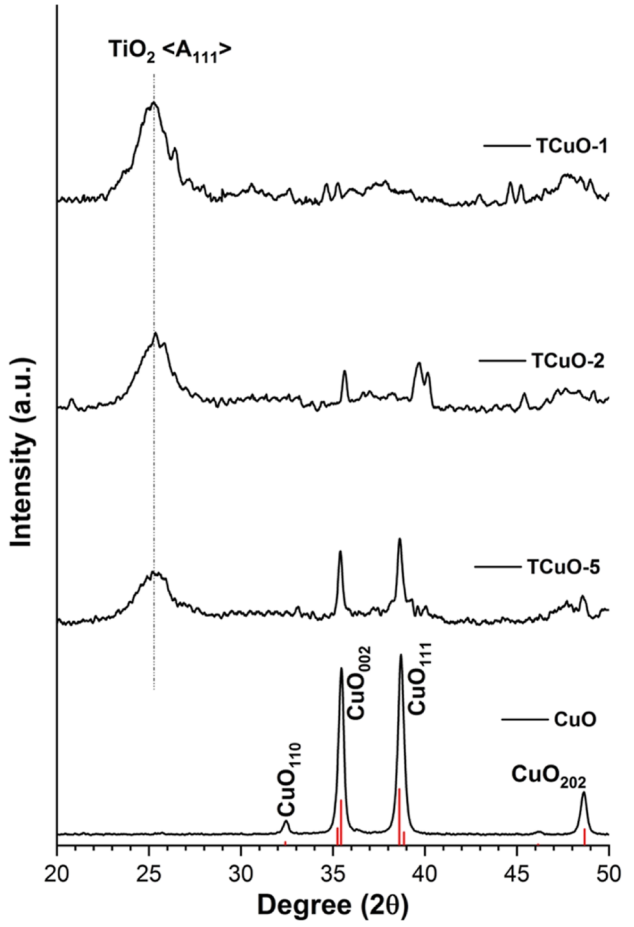

Figure 2. XRD spectra of (bottom to top) CuONPs and TiO_2/CuO coatings; TCuO-5 (5 wt % CuO),TCuO-2 (2 wt % CuO), and TCuO-1 (1 wt % CuO). The red lines represent standard ICDD card.

planes of the corresponding diffraction peaks are assigned that belong to the monoclinic CuO (ICDD-PDF card no. 00-045-0937).[42,43] Diffraction patterns of the CuO/TiO_2 coatings with different CuONP weight percentages are also presented in the figure. Although the diffraction peaks related to CuO NPs are clearly visible in TCuO-5 and TCuO-2 coatings, they are hardly visible in the case of TCuO-1 due to the lower amount of CuONPs present in the coating. All the TiO_2/CuO coatings show a broad diffraction peak centered at about 25.4° 2θ that can be assigned to the anatase phase of TiO_2.[34] The broad nature of the peak suggests poor crystallinity of the TiO_2 coating, which is in agreement that higher temperature is needed to get crystalline TiO_2.[44] The amount of CuO loading in the TiO_2/CuO coatings was estimated from the elemental quantification obtained in the XRF spectra, which is presented in Figure 3. From the quantitative analyses, which are reported in Table 1, the amount of CuO in the CuO/TiO_2 coating was estimated to be about 1, 2, and 5 wt % for TCuO-1, TCuO-2, and TCuO-5 samples, respectively.

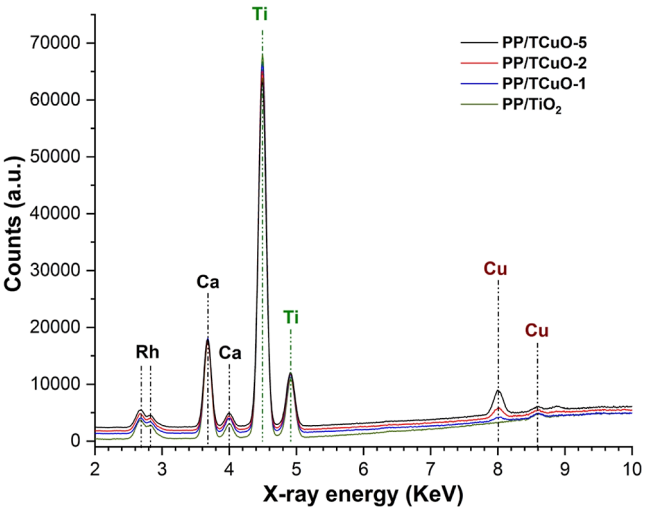

Figure 3. X-ray fluorescence spectra performed on TiO_2-, 1 wt % CuO/TiO_2-, 2 wt % CuO/TiO_2-, and 5 wt % CuO/TiO_2-coated PP substrates. Quantitative estimation of CuO is reported in Table 1.

Figure 4 shows the FESEM images of the coatings with different magnifications. The TiO_2-coated substrate shows a quite smooth surface feature, where the visible microcracks are a common feature in sol−gel-derived coating from the high tension due to shrinkage when the coating thickness exceeds a certain limit.[45,46] From the CuO/TiO_2 coatings, it is observed that CuONPs are uniformly distributed at any CuONP concentration. The most uniform distribution of the CuONPs is observed for TCuO-5 coating. It can also be noticed that in all coatings the CuONPs are well embedded inside the TiO_2 film matrix, suggesting that the CuONPs are not directly exposed to the environment, ensuring that contamination due to the excess release of the CuONPs could be prohibited. On the other hand, even the NPs that remain under the TiO_2 layer could diffuse and interact with the microorganisms through micro- and mesoporous TiO_2 coating, thus making the coating effective against biofilm formation. The adherence of the coatings to the PP substrate was evaluated by the cross-cut tape test method (Figures S1−S3). From the comparison of the optical microscopic images, recorded before and after the cross-cut peeling off test, it is observed that there is merely any peeling off from the coatings, suggesting the coating quality to be 4B according to the ASTM D3359B classification. SEM images taken after the cross-cut test also support these data (Figure S3).

The superhydrophobic nature of the coated surfaces was assessed by measuring the WCA by the sessile drop method reported in Table 1. The bare PP shows a WCA value of 95°, suggesting the hydrophobic (WCA ≥ 90°) nature of the substrate (Figure 5). After TiO_2 spray coating, the WCA value increased to 119° and followed the increasing trend with the loading of CuONPs. The highest WCA value of 160° was obtained for TCuO-5 coating, confirming the superhydrophobic nature of the coated surface. It is expected that high WCA will bring minimal bacterial adhesion and higher antimicrobial activity described in the next section. The higher WCA with an increasing concentration of CuONPs loaded in the coating can be explained by the peculiar surface roughness.[47,48] The dependence of wettability on the surface roughness was determined by the AFM analysis of the coated samples. Figure 6 shows the surface topography of pure TiO_2- and TiO_2/CuO-

https://doi.org/10.1021/acsomega.4c07345
ACS Omega 2024, 9, 45376−45385

Table 1. WCA, Surface Roughness (R_a), and CuO wt % Obtained on Different Coated PP Surfaces

	uncoated/coated PP surfaces				
	PP	PP/TiO_2	PP/TCuO-1	PP/TCuO-2	PP/TCuO-5
WCA[a] (std dev)[b]	95.03 (±1.45)	119.16 (±1.31)	126.08 (±1.43)	133.83 (±1.32)	160.03 (±3.83)
R_a (nm)[c]		24.9 ± 2.5	79.2 ± 3.1	101 ± 2.4	177 ± 4.3
CuO (wt %)[d](std dev)[e]			1.21 (±0.09)	2.25 (±0.11)	5.18 (±0.12)

[a]Average WCA measured on 8 different places. [b]Standard deviation of the 8 measurements. [c]Average surface roughness determined by AFM analyses. [d]Average CuO wt % estimated from the XRF measurements. [e]Standard deviation of the 3 measurements in the area mode.

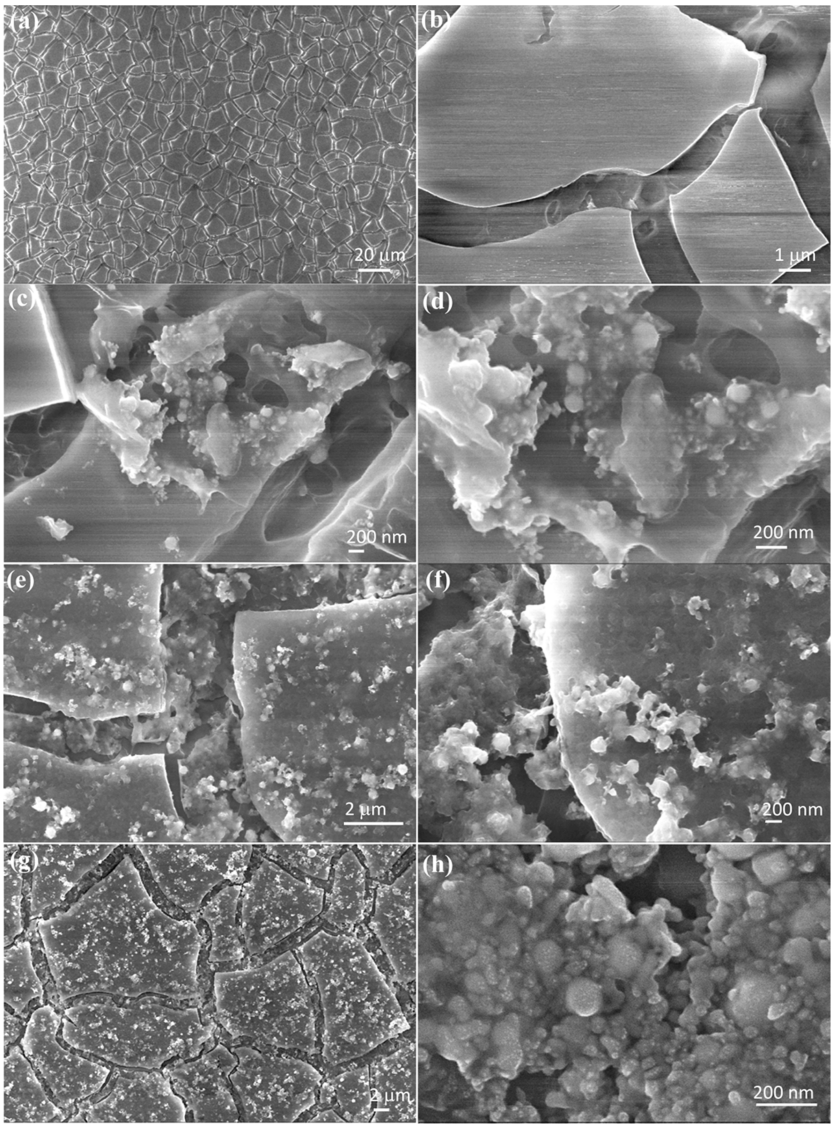

Figure 4. FESEM micrographs with lower and higher magnification of the (a,b) TiO_2-coated PP substrate, (c,d) TCuO-1, (e,f) TCuO-2, and (g,h) TCuO-5.

coated samples, and the average roughness values are reported in Table 1. While a pure TiO_2-coated surface shows an almost smooth morphology with a roughness of 24.9 nm, after CuONPs deposition, the smooth morphology changed to rough surface characteristics with a micronano roughness morphology. This feature is also supported by the FESEM images. The surface roughness increased with the increasing concentration of the CuONPs, achieving the highest value of 177 nm for the TCuO-5 sample (Table 1). This increasing trend of surface roughness with increasing CuONPs concentration is consistent with the increasing WCA values, which changed the wettability behavior of the coatings from hydrophobic to superhydrophobic. Therefore, it could be said that higher surface roughness is responsible for the hydrophobic/superhydrophobic nature of the coatings, as observed by the other researchers.[49,50]

In compliance with the requirements of the ISO 22196:2011 standard, Gram-negative (*E. coli* ATCC 8739) and Gram-positive (*S. aureus* ATCC 6538P) bacterial strains were used to evaluate the antibacterial efficacy of PP/TCuO coatings. Both bacterial strains are widespread pathogens in healthcare facilities, often associated with infections related to medical

https://doi.org/10.1021/acsomega.4c07345
ACS Omega 2024, 9, 45376−45385

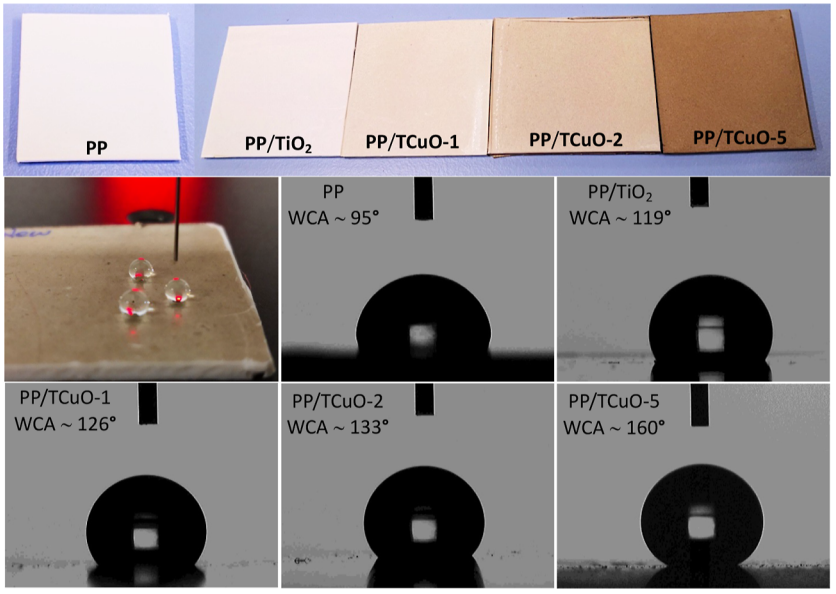

Figure 5. Photographs of the bare PP sheet, TiO_2- and TiO_2/CuO NP-coated PP (top). (Below) photograph of water droplet on the TCuO-5-coated surface and images of the sessile drop on bare and coated PP surfaces. Measured WCA is reported in respective images.

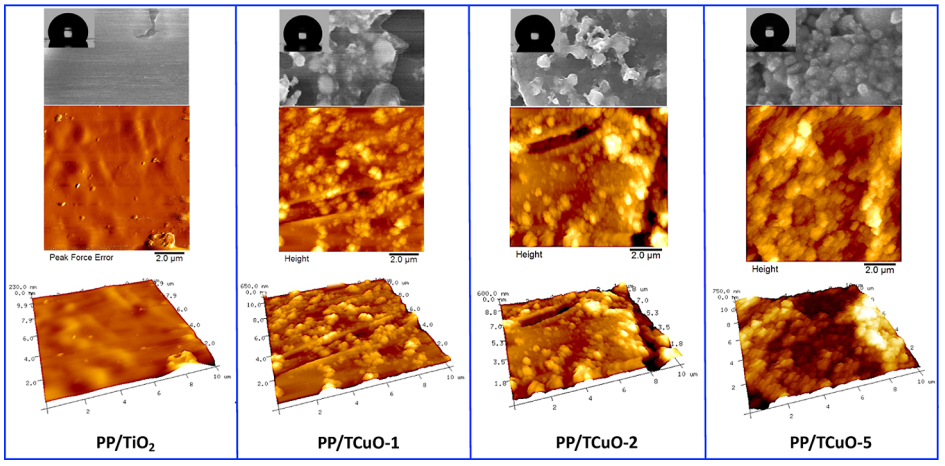

Figure 6. Two-dimensional and three-dimensional AFM images of TiO_2, TCuO-1, TCuO-2, and TCuO-5 coatings on PP substrates. SEM images of the respective samples along with the water droplet (as inset) are shown at the top of each set of micrographs.

devices such as catheters and prosthetic implants.[51,52] Figure 7a,b shows the plot of the number of bacteria inoculated (CFU/cm^2 in Log_{10} scale unit) on coated and uncoated PP substrates against different incubation times for *E. coli* and *S. aureus*, respectively. There was a sharp decrease in the number of bacteria inoculated on TCuO-1 specimen compared to the uncoated one, and no bacterial colony (for both *E. coli* and *S. aureus*) was detected on PCA medium after sowing of bacterial inoculum recovered from the TCuO-2 and TCuO-5 specimens after 24 h of contact. We have also observed a significant decrease in the number of *E. coli* cells recovered from the TCuO-5 specimen immediately after the inoculum at T_0 (data not shown), indicating its strong antimicrobial effect. Figure 7c shows the results of *R* values (estimated from eq 1) against varying concentrations of the CuONPs in the coatings. Referring to ISO 22196:2011, the antibiofilm activity of CuONPs coatings should determine a *R* value ≥2 Log_{10} (CFU/cm^2) within 24 h of incubation. Acceptable *R* values were obtained for the TCuO-1 coating (3.60 and 3.23 for *E. coli* and *S. aureus*, respectively), whereas TCuO-2 (6.03 and 6.11 for *E. coli* and *S. aureus*, respectively) and TCuO-5 (6.49 and 6.31 for *E. coli* and *S. aureus*, respectively) showed much higher *R* values. Reaching an *R* value of higher than 6 for TCuO-2 and TCuO-5 specimens, which corresponds to approximately 99.9999% reduction of the bacterial load, is a very promising result. It is also seen that beyond 2 wt % of CuONPs concentration, there is no significant increment of the *R* value. Therefore, it could be said that 2 wt % CuO concentration could be the ideal candidate for these types of coatings as they would be highly effective in healthcare settings to reduce the microbiological contamination on hospital surfaces. It would also be advantageous to avoid the use of higher concentrations of CuONPs that not only reduce the cost of the process but also elude the risk of environmental hazards. Figure 7d shows the bacterial growth, indicated by the presence or absence of bacterial colonies on PCA medium after the recovery of bacterial cells left in contact with PP- and PP/TCuO-coated specimens for 24 h (T_{24}). Numerous bacterial colonies were detected on the growth medium from the uncoated PP samples, whereas no or very few colonies were

https://doi.org/10.1021/acsomega.4c07345
ACS Omega 2024, 9, 45376−45385

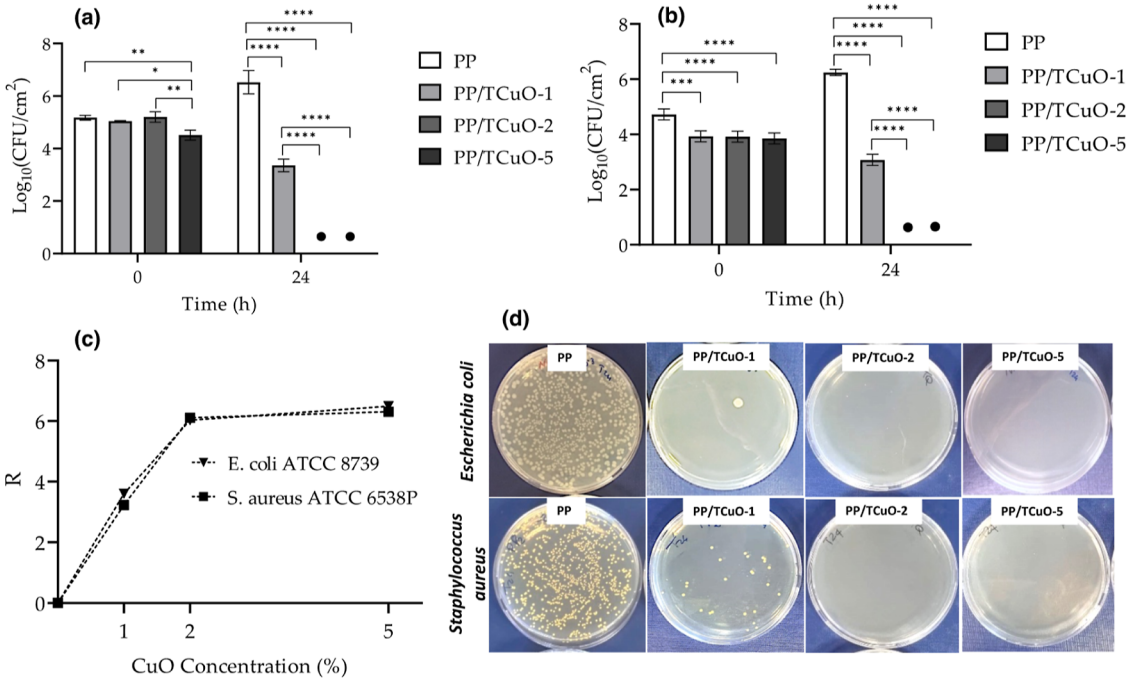

Figure 7. Evaluation of the antibacterial activity of CuONPs coatings on PP specimens against (a) *E. coli* (ATCC 8739) and (b) *S. aureus* (ATCC 6538P); The symbol "•" indicates that no bacterial colony has grown on TCuO-2- and TCuO-5-coating specimens. (c) Estimation of the *R* value with varying concentrations of the CuONPs in the coated specimens. (d) Photographs of the Petri dishes showing the presence and absence of *E. coli* (top) and *S. aureus* (bottom) colonies on PCA medium after the recovery of the bacterial inoculum left in contact with PP- and PP/TCuO-coated specimens for 24 h (T_{24}). *p < 0.05; **p < 0.01; ***p < 0.001; ****p < 0.0001.

observed on the PCA plates when the bacterial suspension was incubated for 24 h in contact with PP/TCuO-coated specimens at different concentrations of CuONPs. Although there are fewer colonies observed with the TCuO-1 specimen (in accordance with obtaining a lower *R* value), no colonies were detected for the TCuO-2 and TCuO-5 specimens. These observations strongly recommend the high bactericidal effect and the antibiofilm activity of the coated films against different types of Gram-negative and Gram-positive bacteria. Although the results highlighted antibiofilm activity, supported by the absence of bacterial cells recovered from the surface of the specimens, the protocol was adapted to verify the presence of nonadherent or dead bacterial cells in a shorter incubation period. The samples were analyzed by SEM, and the results are shown in Figure S4.

Although the killing mechanism of the bacteria by nanoparticles is not straightforward and varies with the type of the particles involved, there is a significant number of studies where the possible bacteria-killing pathways have been proposed, including Cu-based nanomaterials.[2,18,24,26,29,53−55] The antimicrobial and antibiofilm activities of the CuONP-based coatings can be assumed due to one or combined effects of ROS (reactive oxygen species) generation and direct contact of the Cu species with the bacterial cells, often termed the contact killing mechanism. In the former case of ROS generation, highly reactive oxide species such as hydroxyl radicals ($OH^{\bullet}$), superoxide anions ($O_2^{\bullet-}$), singlet oxygen ($^1O_2$), and hydrogen peroxide (H_2O_2) are produced due to the redox reaction between Cu^+ and Cu^{2+} ions either on the surface of the CuONPs or from the dissolution of the Cu ions in biological media.[55,56] These reactive species can induce oxidative stress to proteins, lipids, deoxyribonucleic acid, and other biomolecules, leading to cellular death.[6,26,55,56] In the contact killing mechanism, the positively charged ionic Cu species can directly bind and interact with the negatively charged bacterial cell membrane (for Gram-negative) and cell wall (for Gram-positive), resulting in membrane depolarization that causes the membrane leakage and cell rupture and finally ends up with the destruction of the bacteria. In our case, as there are plenty of CuONPs lying on the coated surface, they can readily interact with the bacterial cell membrane when they come into contact and destroy them according to the above killing mechanisms. This is evidenced from Figure 7, where the log reduction value of >6 (killing efficiency 99.99%) was obtained for both *E. coli* and *S. aureus* with 2 and 5 wt % CuONP-coated specimens. From previous research works, it is revealed that in dry conditions, ROS-mediated antimicrobial activity may not be favorable; instead, contact killing mechanisms would be more effective.[6,56] Since CuONPs are well-known for their toxicity against the microorganisms, it is expected that our coatings would be effective against the biofilm formation in the dry state, which is in fact the real condition of the frequently touched surfaces. Additionally, since the coated surfaces possess superhydrophobicity, they would prevent the bacterial adhesion and act as an antifouling coating.

4. CONCLUSIONS

In this study, we have proposed a high-quality antimicrobial coating preparation that is effective against Gram-positive and Gram-negative pathogenic bacteria. A simple and inexpensive sol−gel spray coating method was used to apply the coatings on PP sheets from CuONPs/TiO_2 sol. Three different coating formulations with different CuONPs/TiO_2 ratios were prepared, and the effect of CuONPs loading on the pathogen killing activity was examined by antimicrobial tests. It is

https://doi.org/10.1021/acsomega.4c07345
ACS Omega 2024, 9, 45376−45385

observed that the antimicrobial activity increases with CuONPs loading, observing the highest antibacterial efficiency with the TCuO-5 coating. Nevertheless, even the lowest concentration investigated in these experiments showed strong antibacterial activity, reaching an R value ≥2 Log_{10} (CFU/cm^2) as required by ISO 22196:2011. The microstructural analyses revealed the incorporation of the CuONPs within the TiO_2 matrix, thus minimizing the environmental risks associated with their release. The superhydrophobic nature of the coatings would additionally protect the coated surface from bacterial/viral adhesion, particularly for those pathogens that are transmitted through the spreading of the droplets. As the CuO/TiO_2 coatings can be applied over a wide range of surfaces, they could be considered as an effective method to protect the high-risk zones from broad-spectrum bacterial infections.

■ ASSOCIATED CONTENT

Supporting Information

The Supporting Information is available free of charge at https://pubs.acs.org/doi/10.1021/acsomega.4c07345.

Characterization methods to assess the coating adherence to the substrate and experimental procedure to test antibiofilm activity; digital photographs of the coated PP sheets with cross-cut; optical micrographs of the coatings before and after the adhesion tape test; SEM images of the coatings after cross-cut adhesion test; and SEM images of *E. coli* and *S. aureus* on CuONPs-coated specimens (PDF)

■ AUTHOR INFORMATION

Corresponding Authors

Sudipto Pal − *Department of Engineering for Innovation, Campus Ecotekne, University of Salento, 73100 Lecce, Italy*; orcid.org/0000-0002-9812-7039; Email: sudipto.pal@unisalento.it

Christian Demitri − *Department of Experimental Medicine, Campus Ecotekne, University of Salento, 73100 Lecce, Italy*; Email: christian.demitri@unisalento.it

Authors

Stefania Villani − *Department of Engineering for Innovation, Campus Ecotekne, University of Salento, 73100 Lecce, Italy*

Antonella Mansi − *Department of Occupational and Environmental Medicine, Epidemiology and Hygiene, National Institute for Insurance against Accidents at Work (INAIL), 00078 Rome, Italy*

Anna Maria Marcelloni − *Department of Occupational and Environmental Medicine, Epidemiology and Hygiene, National Institute for Insurance against Accidents at Work (INAIL), 00078 Rome, Italy*

Alessandra Chiominto − *Department of Occupational and Environmental Medicine, Epidemiology and Hygiene, National Institute for Insurance against Accidents at Work (INAIL), 00078 Rome, Italy*

Ilaria Amori − *Department of Occupational and Environmental Medicine, Epidemiology and Hygiene, National Institute for Insurance against Accidents at Work (INAIL), 00078 Rome, Italy*

Anna Rita Proietto − *Department of Occupational and Environmental Medicine, Epidemiology and Hygiene, National Institute for Insurance against Accidents at Work (INAIL), 00078 Rome, Italy*

Matteo Calcagnile − *Department of Experimental Medicine, Campus Ecotekne, University of Salento, 73100 Lecce, Italy*; orcid.org/0000-0001-9745-4583

Pietro Alifano − *Department of Experimental Medicine, Campus Ecotekne, University of Salento, 73100 Lecce, Italy*; orcid.org/0000-0003-3768-7275

Sonia Bagheri − *Institute of Clinical Physiology, National Research Council, C/o Campus Ecotekne, University of Salento, 73100 Lecce, Italy*

Claudio Mele − *Department of Engineering for Innovation, Campus Ecotekne, University of Salento, 73100 Lecce, Italy*

Antonio Licciulli − *Department of Engineering for Innovation, Campus Ecotekne, University of Salento, 73100 Lecce, Italy*

Alessandro Sannino − *Department of Experimental Medicine, Campus Ecotekne, University of Salento, 73100 Lecce, Italy*

Complete contact information is available at: https://pubs.acs.org/10.1021/acsomega.4c07345

Notes

The authors declare no competing financial interest.

■ ACKNOWLEDGMENTS

This research was supported and funded by the Italian Ministry of University and Research with the Ministerial Decree n. 351/2022—PNRR Mission 4, Component 1, and by the Italian Workers' Compensation Authority (INAIL) within the framework of the project BRIC 2019-ID49.

■ REFERENCES

(1) Solis-Velazquez, O. A.; Gutiérrez-Lomelí, M.; Guerreo-Medina, P. J.; Rosas-García, M. d. L.; Iñiguez-Moreno, M.; Avila-Novoa, M. G. Nosocomial Pathogen Biofilms on Biomaterials: Different Growth Medium Conditions and Components of Biofilms Produced in Vitro. *J. Microbiol., Immunol. Infect.* **2021**, *54* (6), 1038−1047.

(2) Lejeune, B. T.; Zhang, X.; Sun, S.; Hines, J.; Jinn, K. W.; Reilly, A. N.; Clark, H. A.; Lewis, L. H. Enhancing Biocidal Capability in Cuprite Coatings. *ACS Biomater. Sci. Eng.* **2023**, *9* (7), 4178−4186.

(3) Rundle, C. W.; Presley, C. L.; Militello, M.; Barber, C.; Powell, D. L.; Jacob, S. E.; Atwater, A. R.; Watsky, K. L.; Yu, J.; Dunnick, C. A. Hand Hygiene during COVID-19: Recommendations from the American Contact Dermatitis Society. *J. Am. Acad. Dermatol.* **2020**, *83* (6), 1730−1737.

(4) Arnold, W. A.; Blum, A.; Branyan, J.; Bruton, T. A.; Carignan, C. C.; Cortopassi, G.; Datta, S.; DeWitt, J.; Doherty, A.-C.; Halden, R. U.; Harari, H.; Hartmann, E. M.; Hrubec, T. C.; Iyer, S.; Kwiatkowski, C. F.; LaPier, J.; Li, D.; Li, L.; Ortiz, J. G. M.; Salamova, A.; Schettler, T.; Seguin, R. P.; Soehl, A.; Sutton, R.; Xu, L.; Zheng, G. Quaternary Ammonium Compounds: A Chemical Class of Emerging Concern. *Environ. Sci. Technol.* **2023**, *57* (20), 7645−7665.

(5) Zhan, Y.; Yu, S.; Amirfazli, A.; Rahim Siddiqui, A.; Li, W. Recent Advances in Antibacterial Superhydrophobic Coatings. *Adv. Eng. Mater.* **2022**, *24* (4), 2101053.

(6) Mitra, D.; Kang, E.-T.; Neoh, K. G. Antimicrobial Copper-Based Materials and Coatings: Potential Multifaceted Biomedical Applications. *ACS Appl. Mater. Interfaces* **2020**, *12* (19), 21159−21182.

(7) Villani, S.; Kunjalukkal Padmanabhan, S.; Stoppa, M.; Nisi, R.; Calcagnile, M.; Alifano, P.; Demitri, C.; Licciulli, A. Neem-Hypericum-Bacterial Cellulose Wound Care Paste Characterized *in Vitro* and in *Galleria Mellonella in Vivo* Model. *Carbohydr. Polym. Technol. Appl.* **2024**, *7*, 100431.

(8) Yılmaz, G. E.; Göktürk, I.; Ovezova, M.; Yılmaz, F.; Kılıç, S.; Denizli, A. Antimicrobial Nanomaterials: A Review. *Hygiene* **2023**, *3* (3), 269−290.

(9) Imani, S. M.; Ladouceur, L.; Marshall, T.; Maclachlan, R.; Soleymani, L.; Didar, T. F. Antimicrobial Nanomaterials and Coatings: Current Mechanisms and Future Perspectives to Control the Spread of Viruses Including SARS-CoV-2. *ACS Nano* **2020**, *14* (10), 12341−12369.
(10) Liu, S.; Zhang, Z.; Zhang, J.; Qin, G.; Zhang, E. Construction of a TiO2/Cu2O Multifunctional Coating on Ti-Cu Alloy and Its Influence on the Cell Compatibility and Antibacterial Properties. *Surf. Coat. Technol.* **2021**, *421*, 127438.
(11) Ditta, I. B.; Steele, A.; Liptrot, C.; Tobin, J.; Tyler, H.; Yates, H. M.; Sheel, D. W.; Foster, H. A. Photocatalytic Antimicrobial Activity of Thin Surface Films of TiO2, CuO and TiO2/CuO Dual Layers on Escherichia Coli and Bacteriophage T4. *Appl. Microbiol. Biotechnol.* **2008**, *79* (1), 127−133.
(12) Guo, X.; Pan, G.; Fang, L.; Liu, Y.; Rui, Z. Z. Z-Scheme CuOx/Ag/TiO2 Heterojunction as Promising Photoinduced Anticorrosion and Antifouling Integrated Coating in Seawater. *Molecules* **2023**, *28* (1), 456.
(13) Pal, S.; Nisi, R.; Stoppa, M.; Licciulli, A. Silver-Functionalized Bacterial Cellulose as Antibacterial Membrane for Wound-Healing Applications. *ACS Omega* **2017**, *2* (7), 3632−3639.
(14) Zamani, K.; Allah-Bakhshi, N.; Akhavan, F.; Yousefi, M.; Golmoradi, R.; Ramezani, M.; Bach, H.; Razavi, S.; Irajian, G.-R.; Gerami, M.; Pakdin-Parizi, A.; Tafrihi, M.; Ramezani, F. Antibacterial Effect of Cerium Oxide Nanoparticle against Pseudomonas Aeruginosa. *BMC Biotechnol.* **2021**, *21* (1), 68.
(15) Ghezzi, S.; Pagani, I.; Poli, G.; Pal, S.; Licciulli, A.; Perboni, S.; Vicenzi, E. Rapid Inactivation of SARS-CoV-2 by Coupling Tungsten Trioxide (WO3) Photocatalyst with Copper Nanoclusters. *J. Nanotechnol. Nanomater.* **2020**, *1* (3), 109.
(16) Pal, S.; Nisi, R.; Licciulli, A. Antibacterial Activity of In Situ Generated Silver Nanoparticles in Hybrid Silica Films. *Photochem* **2022**, *2* (3), 479−488.
(17) Giedraitienė, A.; Ruzauskas, M.; Šiugždinienė, R.; Tučkutė, S.; Milcius, D. Antimicrobial Properties of CuO Particles Deposited on a Medical Mask. *Materials* **2022**, *15* (22), 7896.
(18) Abraham, J.; Dowling, K.; Florentine, S. Can Copper Products and Surfaces Reduce the Spread of Infectious Microorganisms and Hospital-Acquired Infections? *Materials* **2021**, *14* (13), 3444.
(19) Arendsen, L. P.; Thakar, R.; Sultan, A. H. The Use of Copper as an Antimicrobial Agent in Health Care, Including Obstetrics and Gynecology. *Clin. Microbiol. Rev.* **2019**, *32* (4), No. e00125.
(20) Gallo, N.; Iaconisi, G. N.; Pollini, M.; Paladini, F.; Pal, S.; Nobile, C.; Capobianco, L.; Licciulli, A.; Buonocore, G. G.; Mansi, A.; Salvatore, L.; Sannino, A. Efficacy Evaluation of Cu- and Ag-Based Antibacterial Treatments on Polypropylene Fabric and Comparison with Commercial Products. *Coatings* **2023**, *13* (5), 919.
(21) Michels, H. t.; Noyce, J. o.; Keevil, C. w. Effects of Temperature and Humidity on the Efficacy of Methicillin-Resistant Staphylococcus Aureus Challenged Antimicrobial Materials Containing Silver and Copper. *Lett. Appl. Microbiol.* **2009**, *49* (2), 191−195.
(22) Knobloch, J. K.-M.; Tofern, S.; Kunz, W.; Schütze, S.; Riecke, M.; Solbach, W.; Wuske, T. Life-like" Assessment of Antimicrobial Surfaces by a New Touch Transfer Assay Displays Strong Superiority of a Copper Alloy Compared to Silver Containing Surfaces. *PLoS One* **2017**, *12* (11), No. e0187442.
(23) Hosseini, M.; Chin, A. W. H.; Behzadinasab, S.; Poon, L. L. M.; Ducker, W. A. Cupric Oxide Coating That Rapidly Reduces Infection by SARS-CoV-2 via Solids. *ACS Appl. Mater. Interfaces* **2021**, *13* (5), 5919−5928.
(24) Moniri Javadhesari, S.; Alipour, S.; Mohammadnejad, S.; Akbarpour, M. R. Antibacterial Activity of Ultra-Small Copper Oxide (II) Nanoparticles Synthesized by Mechanochemical Processing against S. Aureus and E. Coli. *Mater. Sci. Eng.: C* **2019**, *105*, 110011.
(25) Kacprzyńska-Gołacka, J.; Łożyńska, M.; Barszcz, W.; Sowa, S.; Wieciński, P.; Woskowicz, E.; Życki, M. Influence of Deposition Parameters of TiO2 + CuO Coating on the Membranes Surface Used in the Filtration Process of Dairy Wastewater on Their Functional Properties. *Membranes* **2021**, *11* (4), 290.
(26) Behzadinasab, S.; Williams, M. D.; Falkinham III, J. O.; Ducker, W. A. Antimicrobial Mechanism of Cuprous Oxide (Cu2O) Coatings. *J. Colloid Interface Sci.* **2023**, *652*, 1867−1877.
(27) Raha, S.; Mallick, R.; Basak, S.; Duttaroy, A. K. Is Copper Beneficial for COVID-19 Patients? *Med. Hypotheses* **2020**, *142*, 109814.
(28) Raship, N. A.; Sahdan, M. Z.; Adriyanto, F.; Nurfazliana, M. F.; Bakri, A. S. Effect of Annealing Temperature on the Properties of Copper Oxide Films Prepared by Dip Coating Technique. *AIP Conf. Proc.* **2017**, *1788* (1), 030121.
(29) Ren, T.; Yang, M.; Wang, K.; Zhang, Y.; He, J. CuO Nanoparticles-Containing Highly Transparent and Superhydrophobic Coatings with Extremely Low Bacterial Adhesion and Excellent Bactericidal Property. *ACS Appl. Mater. Interfaces* **2018**, *10* (30), 25717−25725.
(30) Zhang, X.; Wang, L.; Levänen, E. Superhydrophobic Surfaces for the Reduction of Bacterial Adhesion. *RSC Adv.* **2013**, *3* (30), 12003−12020.
(31) Sahoo, J.; Sarkhel, S.; Mukherjee, N.; Jaiswal, A. Nanomaterial-Based Antimicrobial Coating for Biomedical Implants: New Age Solution for Biofilm-Associated Infections. *ACS Omega* **2022**, *7* (50), 45962−45980.
(32) Varghese, S.; ElFakhri, S. O.; Sheel, D. W.; Sheel, P.; Bolton, F. J. E.; Foster, H. A. Antimicrobial Activity of Novel Nanostructured Cu-SiO2 Coatings Prepared by Chemical Vapour Deposition against Hospital Related Pathogens. *AMB Express* **2013**, *3* (1), 53.
(33) Bharadishettar, N.; Bhat K, U.; Bhat Panemangalore, D. Coating Technologies for Copper Based Antimicrobial Active Surfaces: A Perspective Review. *Metals* **2021**, *11* (5), 711.
(34) Ceglie, C. D.; Pal, S.; Murgolo, S.; Licciulli, A.; Mascolo, G. Investigation of Photocatalysis by Mesoporous Titanium Dioxide Supported on Glass Fibers as an Integrated Technology for Water Remediation. *Catalysts* **2022**, *12* (1), 41.
(35) Leyland, N. S.; Podporska-Carroll, J.; Browne, J.; Hinder, S. J.; Quilty, B.; Pillai, S. C. Highly Efficient F, Cu Doped TiO2 Anti-Bacterial Visible Light Active Photocatalytic Coatings to Combat Hospital-Acquired Infections. *Sci. Rep.* **2016**, *6* (1), 24770.
(36) Alotaibi, A. M.; Williamson, B. A. D.; Sathasivam, S.; Kafizas, A.; Alqahtani, M.; Sotelo-Vazquez, C.; Buckeridge, J.; Wu, J.; Nair, S. P.; Scanlon, D. O.; Parkin, I. P. Enhanced Photocatalytic and Antibacterial Ability of Cu-Doped Anatase TiO2 Thin Films: Theory and Experiment. *ACS Appl. Mater. Interfaces* **2020**, *12* (13), 15348−15361.
(37) Fuentes, S.; Tapia, A.; Pozo, P. Synthesis, Characterization, and Antibacterial Activity Evaluation of Cu@TiO2 Nanocomposites. *Mater. Lett.* **2021**, *296*, 129885.
(38) Wang, C.; Feng, X.; Dan, Y.; Liu, Y.; Li, H. Enhancing Antibacterial Properties and Biosafety Evaluation of TiO2/Cu Photocatalytic Coatings Through Suspension Flame Spraying. *J. Therm. Spray Technol.* **2024**, *33* (1), 101−112.
(39) Sondezi, N.; Njengele-Tetyana, Z.; Matabola, K. P.; Makhetha, T. A. Sol−Gel-Derived TiO2 and TiO2/Cu Nanoparticles: Synthesis, Characterization, and Antibacterial Efficacy. *ACS Omega* **2024**, *9* (14), 15959−15970.
(40) *ISO 22196:2011 Measurement of antibacterial activity on plastics and other non-porous surfaces.* https://www.iso.org/standard/54431.html (accessed 10 30, 2023).
(41) *ISO 846:1997(en), Plastics—Evaluation of the action of microorganisms.* https://www.iso.org/obp/ui/en/#iso:std:iso:846:ed-2:v1:en (accessed 10 30, 2023).
(42) Gao, P.; Liu, D. Facile Synthesis of Copper Oxide Nanostructures and Their Application in Non-Enzymatic Hydrogen Peroxide Sensing. *Sens. Actuators, B* **2015**, *208*, 346−354.
(43) Riad, K. B.; Hoa, S. V.; Wood-Adams, P. M. Metal Oxide Quantum Dots Embedded in Silica Matrices Made by Flame Spray Pyrolysis. *ACS Omega* **2021**, *6* (17), 11411−11417.
(44) Pal, S.; Laera, A. M.; Licciulli, A.; Catalano, M.; Taurino, A. Biphase TiO2Microspheres with Enhanced Photocatalytic Activity. *Ind. Eng. Chem. Res.* **2014**, *53* (19), 7931−7938.

https://doi.org/10.1021/acsomega.4c07345
ACS Omega 2024, 9, 45376−45385

(45) Licciulli, A.; Riccardis, A. D.; Pal, S.; Nisi, R.; Mele, G.; Cannoletta, D. Ethylene Photo-Oxidation on Copper Phthalocyanine Sensitized TiO2 Films under Solar Radiation. *J. Photochem. Photobiol., A* **2017**, *346*, 523−529.
(46) Kappert, E. J.; Pavlenko, D.; Malzbender, J.; Nijmeijer, A.; Benes, N. E.; Tsai, P. A. Formation and Prevention of Fractures in Sol−Gel-Derived Thin Films. *Soft Matter* **2015**, *11* (5), 882−888.
(47) Hong, H. R.; Kim, J. Nanoroughness-Mediated Bacterial Adhesion on Fabrics. *ACS Appl. Nano Mater.* **2023**, *6* (19), 18518−18530.
(48) Parvate, S.; Dixit, P.; Chattopadhyay, S. Superhydrophobic Surfaces: Insights from Theory and Experiment. *J. Phys. Chem. B* **2020**, *124* (8), 1323−1360.
(49) Manoudis, P. N.; Karapanagiotis, I.; Tsakalof, A.; Zuburtikudis, I.; Panayiotou, C. Superhydrophobic Composite Films Produced on Various Substrates. *Langmuir* **2008**, *24* (19), 11225−11232.
(50) Zhang, S.; Liang, X.; Gadd, G. M.; Zhao, Q. Superhydrophobic Coatings for Urinary Catheters To Delay Bacterial Biofilm Formation and Catheter-Associated Urinary Tract Infection. *ACS Appl. Bio Mater.* **2020**, *3* (1), 282−291.
(51) Pietrocola, G.; Campoccia, D.; Motta, C.; Montanaro, L.; Arciola, C. R.; Speziale, P. Colonization and Infection of Indwelling Medical Devices by Staphylococcus Aureus with an Emphasis on Orthopedic Implants. *Int. J. Mol. Sci.* **2022**, *23* (11), 5958.
(52) Sharma, G.; Sharma, S.; Sharma, P.; Chandola, D.; Dang, S.; Gupta, S.; Gabrani, R. Escherichia Coli Biofilm: Development and Therapeutic Strategies. *J. Appl. Microbiol.* **2016**, *121* (2), 309−319.
(53) Tamayo, L.; Azócar, M.; Kogan, M.; Riveros, A.; Páez, M. Copper-Polymer Nanocomposites: An Excellent and Cost-Effective Biocide for Use on Antibacterial Surfaces. *Mater. Sci. Eng.: C* **2016**, *69*, 1391−1409.
(54) Fu, Y.; Chang, F.-M. J.; Giedroc, D. P. Copper Transport and Trafficking at the Host−Bacterial Pathogen Interface. *Acc. Chem. Res.* **2014**, *47* (12), 3605−3613.
(55) Angelé-Martínez, C.; Nguyen, K. V. T.; Ameer, F. S.; Anker, J. N.; Brumaghim, J. L. Reactive Oxygen Species Generation by Copper(II) Oxide Nanoparticles Determined by DNA Damage Assays and EPR Spectroscopy. *Nanotoxicology* **2017**, *11* (2), 278−288.
(56) Borkow, G. Using Copper to Fight Microorganisms. *Curr. Chem. Biol.* **2012**, *6* (2), 93−103.

https://doi.org/10.1021/acsomega.4c07345
ACS Omega 2024, 9, 45376−45385